Transcriptional Regulation of miR528 by OsSPL9 Orchestrates Antiviral Response in Rice

Shengze Yao[1,6], Zhirui Yang[1,6], Rongxin Yang[2], Yu Huang[1], Ge Guo[1], Xiangyue Kong[1], Ying Lan[3], Tong Zhou[3], He Wang[4], Wenming Wang[4], Xiaofeng Cao[2], Jianguo Wu[5,*] and Yi Li[1,*]

[1]The State Key Laboratory of Protein and Plant Gene Research, School of Life Sciences, Peking University, Beijing 100871, China

[2]State Key Laboratory of Plant Genomics and National Center for Plant Gene Research, Institute of Genetics and Developmental Biology, Chinese Academy of Sciences, Beijing 100101, China

[3]Institute of Plant Protection, Jiangsu Academy of Agricultural Sciences, Nanjing 210014, China

[4]Rice Research Institute and College of Agronomy, Sichuan Agricultural University, Chengdu 611130, China

[5]Vector-borne Virus Research Center, State Key Laboratory for Ecological Pest Control of Fujian and Taiwan Crops, College of Plant Protection, Fujian Agriculture and Forestry University, Fuzhou 350002, China

[6]These authors contributed equally to this article.

*Correspondence: Jianguo Wu (wujianguo81@126.com), Yi Li (liyi@pku.edu.cn)

https://doi.org/10.1016/j.molp.2019.04.010

ABSTRACT

Many microRNAs (miRNAs) are critical regulators of plant antiviral defense. However, little is known about how these miRNAs respond to virus invasion at the transcriptional level. We previously show that defense against *Rice stripe virus* (RSV) invasion entailed a reduction of miR528 accumulation in rice, alleviating miR528-mediated degradation of *L-Ascorbate Oxidase* (*AO*) mRNA and bolstering the antiviral activity of AO. Here we show that the *miR528-AO* defense module is regulated by the transcription factor SPL9. SPL9 displayed high-affinity binding to specific motifs within the promoter region of miR528 and activated the expression of miR528 gene *in vivo*. Loss-of-function mutations in *SPL9* caused a significant reduction in miR528 accumulation but a substantial increase of *AO* mRNA, resulting in enhanced plant resistance to RSV. Conversely, transgenic overexpression of *SPL9* stimulated the expression of miR528 gene, hence lowering the level of *AO* mRNA and compromising rice defense against RSV. Importantly, gain in RSV susceptibility did not occur when *SPL9* was overexpressed in *mir528* loss-of-function mutants, or in transgenic rice expressing a miR528-resistant *AO*. Taken together, the finding of SPL9-mediated transcriptional activation of miR528 expression adds a new regulatory layer to the *miR528-AO* antiviral defense pathway.

Key words: SPL9, miR528, Antiviral defence, Rice

INTRODUCTION

Insect-transmitted viruses constitute a major threat to rice productivity and, thus, worldwide food security (Wu et al., 2015, 2017; Zhang et al., 2016; Tang and Chu, 2017). To tackle this problem, we have been using *Rice stripe virus* (RSV), which is transmitted by the small brown planthopper (*Laodelphax striatellus*), as a model to unravel antiviral defense mechanisms in rice that can be harnessed to combat rice virus epidemics (Du et al., 2011; Wang et al., 2014). RNA silencing is an evolutionarily conserved mechanism of antiviral defense that is well studied in model dicot plants and other eukaryotes, but is not well understood in economically important crops (Baumberger et al., 2007; Diaz-Pendon et al., 2007; Brosseau and Moffett, 2015; Sanei and Chen, 2015; Fang and Qi, 2016;

Ma and Zhang, 2018). The components of RNA silencing including AGO, DCL, RDR, small interfering RNA, microRNA (miRNA), and other elements play critical roles in plant–virus interactions (Qu et al., 2008; Carbonell and Carrington, 2015; Huang and Li, 2018; Yang and Li, 2018; Guo et al., 2019). Recently, there have been many important advances in identifying miRNA–pathogen interactions, such as miR159-MYB, miR164-NAC, miR169-NFYA, miR319-TCP, miR393-TIR1, miR398-CSD, miR393*-MEBM12, miR444-MADS, miR482-*R* genes, and miR9836-MLA1 (Navarro et al., 2006; Zhang et al., 2011, 2016; Du et al., 2014; Liu et al., 2014;

Ouyang et al., 2014; Xu et al., 2014; Hanemian et al., 2016; Wang et al., 2016, 2018b). However, little is known about how these miRNAs respond to pathogen invasion at the transcriptional level. Our previous work revealed the complex interplay between RSV infection and the RNA-silencing pathways in rice that determine infection outcomes. Relevant to the current study is the intriguing role played by the rice Argonaute 18 (AGO18) in sequestering a subset of miRNAs. Specifically, sequestration of miR168 and miR528 by AGO18 during RSV infection relieved *AGO1* and *L-Ascorbate Oxidase* (*AO*), respectively, from miRNA-mediated degradation, allowing them to exert their antiviral functions (Wu et al., 2015, 2017). These and other reports suggest that many miRNAs act as pivotal modulators of plant antiviral immune responses by regulating the turnover of immunity-associated targets (Zheng et al., 2017). Consistent with this idea, we showed that RSV infection perturbed the accumulation of many miRNAs. In particular, the expression of miR528 was dramatically downregulated (Wu et al., 2017). However, the molecular mechanisms regulating expression of miR528 gene remain unclear. In this study, we found that SPL9 specifically activates the transcription of miR528 gene and orchestrates the antiviral response in rice.

RESULTS

SPL9 Specifically Activates the Transcription of miR528 Gene among 19 Rice SPL Transcription Factors

To identify the transcriptional factor regulating the expression of miR528 gene, we first analyzed the promoter sequence of miR528 using the online software PlantCare and New PLACE (Supplemental Data 4), and identified a large number of GTAC motifs (Supplemental Figure 1A). GTAC motifs are known to be the binding sites of transcription factors belonging to the SQUAMOSA Promoter Binding Protein-Like (SPL) family (Xie et al., 2006; Yamasaki et al., 2009; Wang et al., 2018a). Therefore, we next asked whether any of the 19 SPLs encoded in the rice genome regulate miR528 transcription (Xie et al., 2006) (Supplemental Figure 1B). To this end, we first used the yeast-one-hybrid (Y1H) assay to determine which rice SPL(s) binds the miR528 promoter specifically in yeast cells.

The promoter region of miR528 was cloned into the *pHis2* vector to form a reporter construct, and the coding sequences of 19 rice SPLs were fused with the yeast activation domain (AD) (*pGADT7Rec2*) to form the effector constructs AD-SPL1 to AD-SPL19 (Supplemental Figure 2A). Surprisingly, only SPL9 was able to bind to the miR528 promoter and activate the transcription of the downstream *His3* reporter gene (Supplemental Figure 2B). Consistent with this result, the expression level of *pre-miR528* was unchanged in transgenic plants overexpressing miR156, where 10 out of the 19 rice *SPL*s (*SPL2–4*, *SPL7*, *SPL11–14*, *SPL17*, *SPL18*) were downregulated as a result of enhanced miR156-mediated mRNA degradation (Xie et al., 2006). Similarly, no change in *pre-miR528* levels was detected in rice lines harboring loss-of-function mutations in *SPL1* and *SPL12* (introduced with CRISPR/Cas9), or *SPL6* (Tos17 insertion) (Wang et al., 2018a) (Supplemental Figure 3).

SPL9 Binds the Promoter of miR528 Gene and Activates Its Transcription

We next tested whether miR528 accumulation is under direct regulation by SPL9. To accomplish this, we generated rice lines in which SPL9 is either overexpressed (the *SPL9 OE* lines), or knocked out (with CRISPR/Cas9) (Supplemental Figure 4A–4C). Neither manipulation caused visible alteration in rice-growth behavior or appearance (Supplemental Figure 4D). We first measured the miR528 levels in these rice lines using quantitative reverse transcription PCR (qRT–PCR). Both *pre-miR528* and mature miR528 were significantly upregulated in *SPL9 OE* rice lines (Figure 1A and Supplemental Figure 5A), but significantly downregulated in *spl9* knockout lines (Figure 1B and Supplemental Figure 5B).

We speculated that SPL9 could bind to the GTAC motifs within the promoter region of the miR528 gene and activate its transcription. To test this, we used the dual-luciferase reporter system and Y1H assay to assess whether mutations in these GTAC motifs compromise SPL9-dependent transcription of the miR528 promoter. The mutated miR528 promoter, in which all GTAC motifs were changed to GATC, lost the ability to be activated by SPL9 (Figure 1C and Supplemental Figure 5C–5E). The direct interaction between SPL9 and the miR528 promoter was subsequently demonstrated *in vitro* using an electrophoretic mobility shift assay (EMSA). To this end, the SPL9 DNA-binding domain (SBP, ca. 33kDa) was fused with glutathione *S*-transferase (GST), and the GST-SPL9 SBP fusion protein was expressed in *Escherichia coli* and purified (Supplemental Figure 5F). As shown in Figure 1E, the band corresponding to a region of the miR528 promoter harboring GTAC motifs shifted dramatically upwards indicating strong DNA-SPL9 binding. Importantly, this binding was impaired by the addition of a cold competitor probe containing the same sequence, but not by the mutated probe in which GTAC was changed to GATC. Additionally the recognition of GTAC motifs by GST-SPL9 SBP was also demonstrated using the microscale thermophoresis (MST) assay; GST-SPL9 SBP bound to a region of the miR528 promoter containing the GTAC motif with a binding constant of $12\ 921 \pm 784.95$ nM (Supplemental Figure 5G).

Finally, to confirm the specific interaction between SPL9 and the miR528 promoter in rice plants, we immunoprecipitated the chromatin extracts of *SPL9 OE* rice lines (expressing SPL fused with an FLAG tag) with an FLAG antibody, and quantified the presence of miR528 promoter DNA in the precipitates using chromatin immunoprecipitation coupled with qPCR (ChIP–qPCR) (Figure 1F). The results of the ChIP–qPCR experiment revealed a significant enrichment of miR528 promoter sequence, and hence the high-affinity interaction of SPL9 and the miR528 promoter in rice plants. Taken together, our data demonstrate that SPL9 activates the transcription of miR528.

SPL9 Regulates the Expression of *AO*, a Target Gene of miR528

Our previous study showed that miR528 participates in rice antiviral defense by regulating the expression of the target gene, *AO*. The fact that SPL9 controls the transcription of miR528 led us to
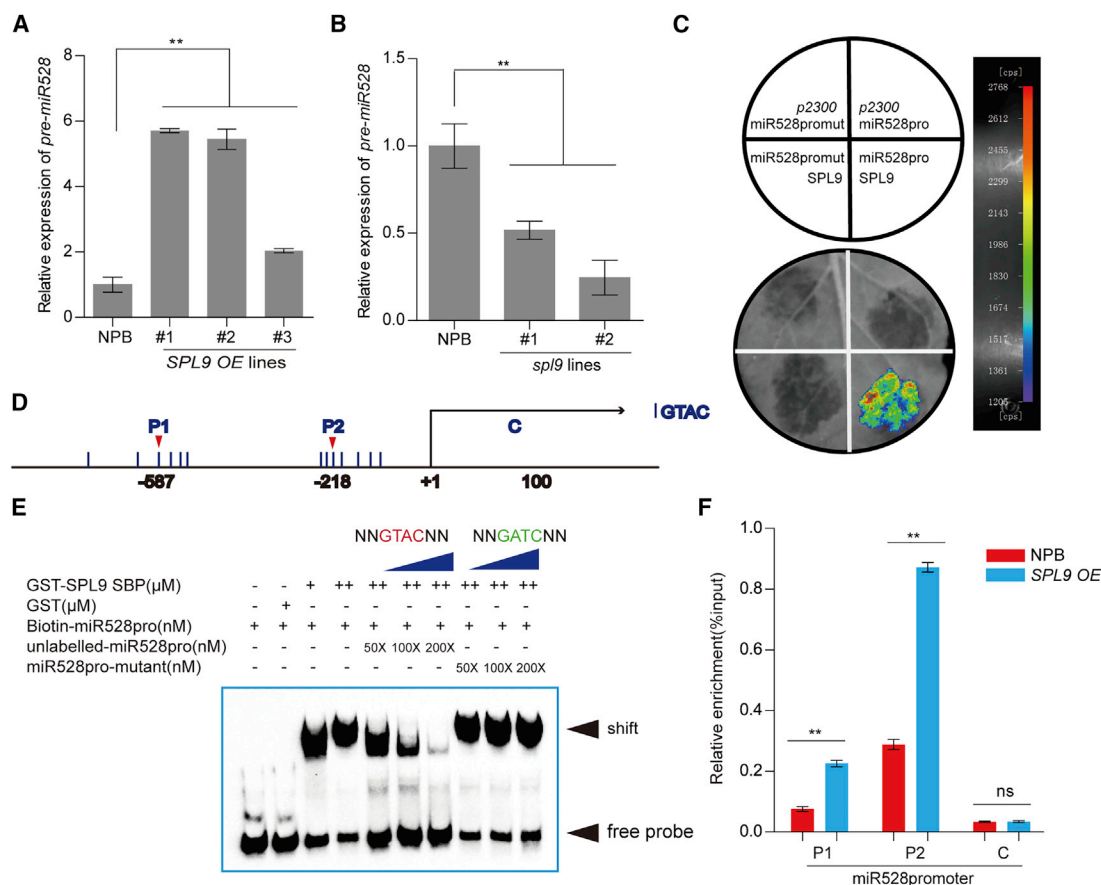
Figure 1. SPL9 Positively Controls miR528 Transcription by Binding to GTAC Motifs in the miR528 Promoter.

(A and B) qRT–PCR analysis of the expression levels of *pre-miR528* in the wild-type (NPB) and *SPL9 OE* **(A)** and *spl9* mutant **(B)** lines. The average values (±SD) from three biological repeats are shown. Asterisks mark significant differences from the wild type, according to Student's *t*-test: **$P \leq 0.01$.

(C) A luciferase imaging assay shows that SPL9 activates miR528 transcription in *N. benthamiana* leaves. *Agrobacterium* strain GV3101 harboring different construct combinations (*pCambia2300*, *pCambia2300-SPL9*, *pGreenII 0800-LUC*-miR528pro, *pGreenII 0800-LUC*-miR528pro mut) was infiltrated into different *N. benthamiana* leaf regions. Two days after infiltration, luciferase activities were recorded in these regions. cps indicates signal counts per second.

(D) Schematic diagram of the miR528 promoter. The potential SPL9 binding sites are shown. The numbers below the diagram indicate the distance away from the translational start site, ATG (+1). P1 and P2 indicate the DNA fragments used for ChIP–qPCR.

(E) Electrophoretic mobility shift assays of the binding of SPL9 to a GTAC motif in the miR528 promoter. A biotinylated probe containing the GTAC motif sequence was incubated with the GST-fused SPL9 DNA-binding domain (GST-SPL9 SBP), while the probe incubated with no protein or GST protein was used as a negative control. Nonlabeled probes NNGTACNN and NNGATCNN were used as cold competitors and mutant competitors, respectively.

(F) ChIP–qPCR assays showing that SPL9 binds to the promoter of miR528 *in vivo*. The immunoprecipitation of FLAG-tagged SPL9 from *SPL9 OE* plants was performed using an anti-FLAG antibody. Immunoprecipitated chromatin was analyzed using qRT–PCR. The primers (P1 and P2) used in the assays are indicated in the schematic diagram of the miR528 promoter **(D)**. The enrichment was normalized to the actin levels and the total input of each sample. Segment C (located in the coding region) was used as the negative control. The average values (±SD) from three biological repeats are shown. Asterisks mark significant differences from the wild type, according to Student's *t*-test: **$P \leq 0.01$; ns, no significant difference.

predict that the *AO* mRNA levels would also change in *SPL9 OE* and *spl9* rice lines. Indeed, the accumulation of *AO* decreased in *SPL9 OE* lines (Figure 2A and 2B) at both the mRNA and protein levels, and increased in *spl9* knockout lines (Figure 2C and 2D). Therefore, SPL9 indirectly regulates *AO* expression by transcriptionally regulating miR528.

SPL9 Negatively Regulates Rice Antiviral Response to RSV Infection

Would the reduction of AO levels in *SPL9 OE* lines weaken rice defense against RSV? To answer this question, we inoculated seedlings of the *SPL9 OE* lines and the *spl9* knockout lines

with RSV using viruliferous brown planthoppers *L. striatellus*. The wild-type rice cultivar Nipponbare (NPB) was used as the control. Compared with NPB, the *SPL9 OE* lines exhibited more severe symptoms and higher disease incidence (Figure 3A, Supplemental Figure 6C, and Supplemental Data 1A), whereas the *spl9* lines showed much milder symptoms and lower disease incidence (Figure 3D, Supplemental Figure 6D, and Supplemental Data 1B). The accumulation of RSV genome segments RNA1 and RNA3 was assessed by qRT–PCR, and that of RSV coat protein (CP) was assayed by western blot. Levels of RSV RNAs and CP were both elevated in the *SPL9 OE* lines (Figure 3B and 3C; Supplemental Figure 6A), but decreased in *spl9* mutants
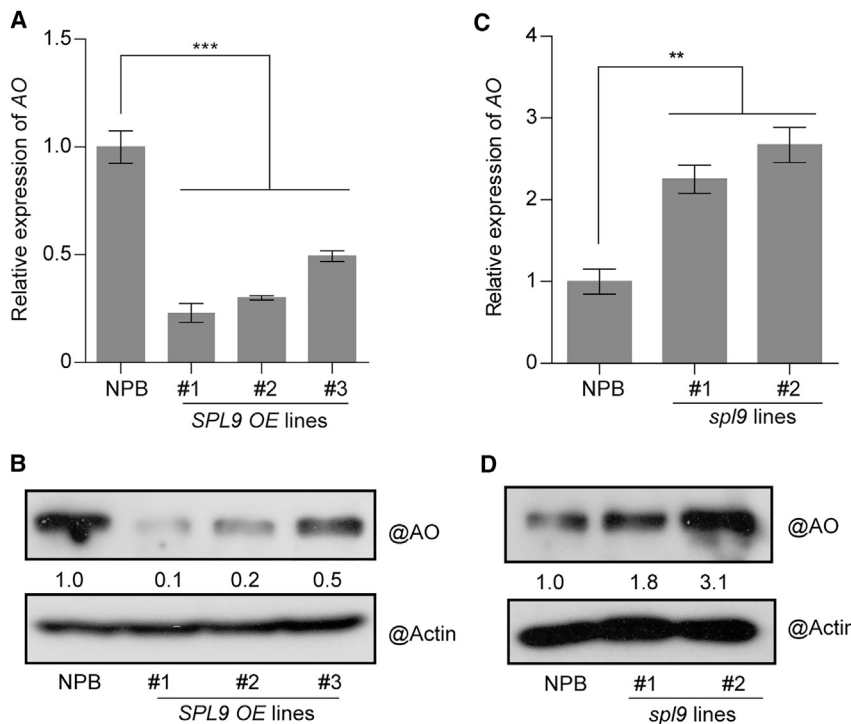
Figure 2. SPL9 Negatively Regulates the Expression of *AO*.

(A) qRT–PCR analysis of *AO* expression in the wild-type (NPB) and *SPL9 OE* lines. The average values (±SD) from three biological repeats are shown. Asterisks mark significant differences from the wild type, according to Student's *t*-test: ***$P \leq 0.001$.

(B) Detection of AO protein levels in NPB and *SPL9 OE* using a western blot. Actin was probed as a loading control.

(C) qRT–PCR analysis of the expression level of *AO* in NPB and *spl9* mutant lines. The average values (±SD) from three biological repeats are shown. Asterisks mark significant differences from the wild type, according to Student's *t*-test: **$P \leq 0.01$.

(D) Detection of the AO protein levels in NPB and *spl9* mutant lines using a western blot. Actin was probed as a loading control.

(Figure 3E and 3F; Supplemental Figure 6B). Thus, overexpression of *SPL9* compromised rice defense against RSV, whereas inactivation of *SPL9* enhanced this defense. In short, SPL9, by stimulating miR528 expression, negatively regulates rice antiviral response.

SPL9 Regulates Rice Antiviral Defense through the *miR528-AO* Module

To further demonstrate that *SPL9* acts through miR528, we next attempted to overexpress *SPL9* in *mir528* mutant rice (*Dongjin*, DJ background) in which the *miR528* gene was knocked out. The resultant *SPL9 OE/mir528* lines accumulated more SPL9 at both the mRNA and protein levels, but displayed normal growth and development (Supplemental Figure 7A). In contrast to *SPL9 OE* lines, which contained less AO mRNA and protein, the new *SPL9 OE/mir528 SPL9* lines accumulated higher levels of *AO* mRNA and protein due to the loss of miR528-mediated mRNA degradation (Figure 4A and 4B). Furthermore, while SPL9 overexpression alone (the *SPL9 OE* lines) led to increased susceptibility to RSV infection, its overexpression in the absence of miR528 (the new *SPL9 OE/mir528* lines) had no effect on RSV susceptibility when compared with the *mir528* knockout lines (the increased resistance over the wild-type control was due to the lack of miR528 function) (Figure 4C). These results were verified with assays that measured the levels of RSV genomic RNA1, RNA3, and RSV-CP (Figure 4D and Supplemental Figure 7B), as well as the infection rates in each rice line (Supplemental Figure 7C and Supplemental Data 1C).

Similar results were obtained when *SPL9* was overexpressed in *AO-Res* lines, in which the *AO* gene was mutated at the miR528 target site to permit the escape from miR528-mediated mRNA degradation (Wu et al., 2017). These *AO-Res* lines contained higher levels of *AO* mRNA and protein than wild-type rice, and were more resistant to RSV infection (Wu et al., 2017). Overexpression of *SPL9* in the *AO-Res* background (the *SPL9 OE/AO-Res* lines), while elevating the levels of miR528, failed to decrease the levels of AO or enhance RSV susceptibility (Supplemental Figure 8). Together our data clearly demonstrate that SPL9 regulates rice defense against RSV through the *miR528-AO* module.

DISCUSSION

In the current study we identified SPL9, a rice transcription factor (TF) that stimulates the transcription of miR528 and, through the miR528-mediated regulation of *AO* expression, orchestrates the defense response to RSV infection. MiR528 is specifically regulated by SPL9 among the 19 rice SPLs (Supplemental Figure 2 and Figure 1). SPL-specific regulation of targets was also demonstrated for other SPL TFs. For example, in the IPA1 (SPL14)-WRKY45, SPL6-IRE1, and SPL16-GW7 modules different SPLs drive different downstream pathways to play roles in rice growth, development, and response to pathogens (Wang et al., 2015, 2018a, 2018c). It is well known that TFs from the same family usually bind the same motif in the promoters of their target genes, but this does not mean that a promoter with the same motif will be regulated by all TFs in the same family. There are several possible reasons for this TF-specific regulation. First, there might be some co-factors that interact directly or indirectly with specific TFs and form a specific regulation complex; second, specific structures in the promoter of the target gene may determine TF-specific regulation; and third, the temporal and spatial expression of TFs and their targets must be taken into account.

Based on our genetic and viral infection assays (Figure 4 and Supplemental Figure 8), in the *miR528-AO* module, *SPL9* mainly participates in the response to viral infection. Although SPL9 is a positive regulator of miR528 transcription, its role in antiviral defense is clearly negative (Figures 1 and 3). MiR528 targets not only
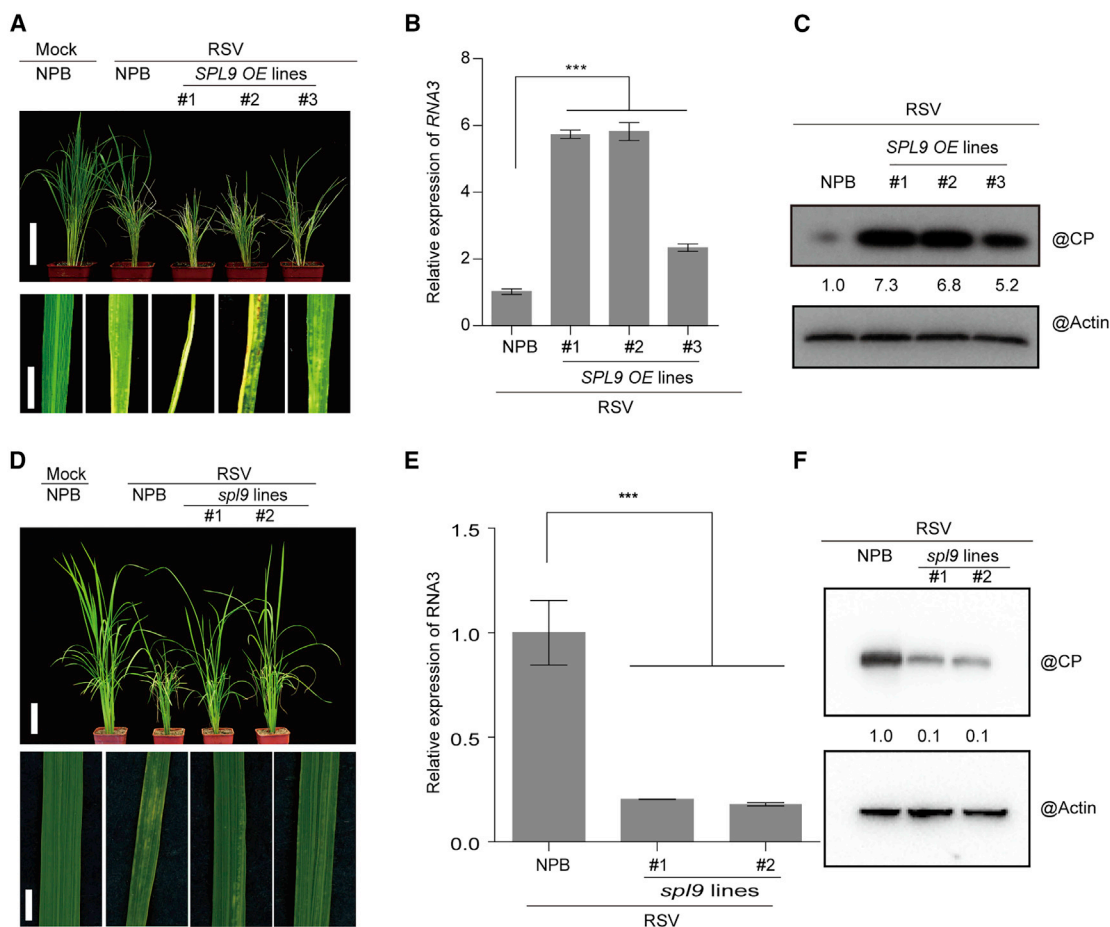
Figure 3. SPL9 Negatively Regulates Rice Resistance to RSV Infection.

(A) Symptoms of the mock-inoculated wild-type (NPB) and RSV-infected NPB and *SPL9 OE* lines at 4 weeks post inoculation (wpi). Scale bars, 10 cm (upper panel) and 1 cm (lower panel).

(B) qRT–PCR analysis of the expression level of *RSV-RNA3* in NPB and *SPL9 OE* lines. The average values (±SD) from three biological repeats are shown. Asterisks mark significant differences from the wild type, according to Student's *t*-test: **$P \leq 0.01$.

(C) Detection of RSV-CP proteins in NPB and *SPL9 OE* lines using a western blot. Actin was probed as a loading control.

(D) Symptoms of the mock-inoculated NPB and RSV-infected NPB and *spl9* lines at 4 wpi. Scale bars, 10 cm (upper panel) and 1 cm (lower panel).

(E) qRT–PCR analysis of the expression level of *RSV-RNA3* in NPB and *spl9* lines. The average values (±SD) from three biological repeats are shown. Asterisks mark significant differences from the wild type, according to Student's *t*-test: ***$P \leq 0.001$.

(F) Detection of RSV-CP in NPB and *spl9* lines using a western blot. Actin was probed as a loading control.

the *AO* gene but also plastocyanin-like proteins and EIN3-binding F-box protein; therefore, SPL9-miR528 may regulate other processes in rice growth and development. Since an overly active defense response is known to be detrimental to plant survival, we speculate that SPL9 may act to balance the needs of defense and growth.

How SPL9 is regulated upon RSV infection is an interesting question. To address this issue, we measured the mRNA and protein levels of *SPL9* by qRT–PCR and western blot, respectively, after RSV infection. The results showed that *SPL9* was obviously downregulated at the protein level while there were no significant changes at the mRNA level (Figure 5A and 5B), which means that translational suppression, post-translational modification, or degradation of the SPL9 protein may take place via an unknown mechanism under RSV infection. These open questions need further investigation (Figure 5C).

METHODS

Plant Growth and Virus Inoculation

Rice (*Oryza sativa* spp. *japonica*) plants were grown and inoculated with RSV as previously described (Wu et al., 2015, 2017). In brief, the rice seedlings were grown in a glasshouse at 28°C–30°C for 2 weeks before being inoculated with viruliferous (RSV) or virus-free (mock) insects (*Laodelphax striatellus*) for 2 days. The insects were then removed and the rice seedlings were grown in the glasshouse under a 14:10-h light/dark photoperiod at 28°C during the day and 25°C at night. The number of plants with viral symptoms in each line was recorded each week (Supplemental Data 1). The plants were photographed and harvested at 4 weeks post inoculation. At least 30 rice plants per line were used.

Phylogenetic Analysis

The amino acid sequences of the rice SPL family proteins were obtained from UniProt. A maximum-likelihood tree was constructed using MEGA 7.
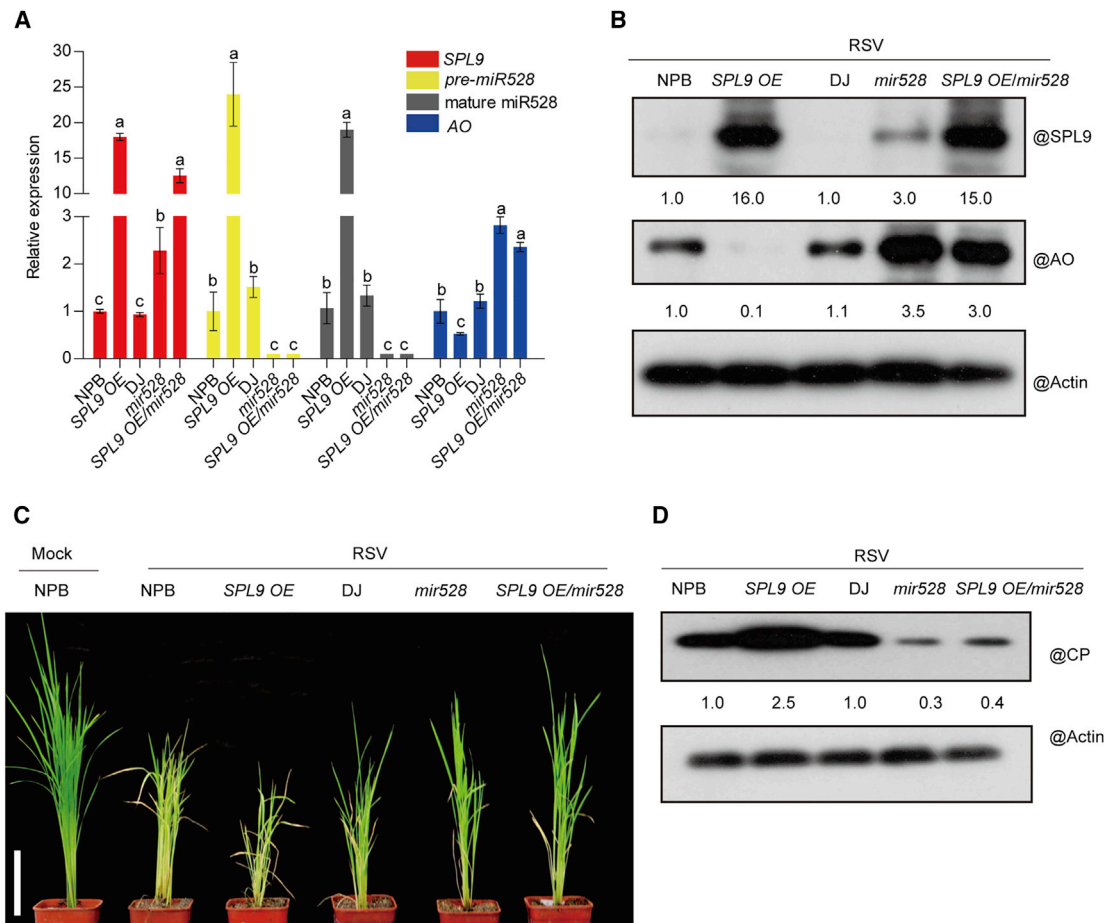
Figure 4. SPL9 Regulates RSV Infection through the *miR528-AO* Pathway.

(A) qRT–PCR analysis of the expression levels of *SPL9*, *pre-miR528*, mature miR528, and *AO* in the wild-type (NPB and DJ), *SPL9 OE*, *mir528*, and *SPL9 OE/mir528* lines. The average values (±SD) from three biological repeats are shown. For each gene, different letters indicate significant differences in expression according to Student's *t*-test: $P \leq 0.05$.

(B) Detection of SPL9 and AO levels in the wild-type (NPB and DJ), *SPL9 OE*, *mir528*, and *SPL9 OE/mir528* lines using a western blot. Actin was probed as a loading control.

(C) Symptoms of the mock-inoculated wild-type (NPB) and RSV-infected wild-type (NPB and DJ), *SPL9 OE*, *mir528*, and *SPL9 OE/mir528* lines at 4 wpi. Scale bars, 10 cm.

(D) Detection of RSV-CP in wild-type (NPB and DJ), *SPL9 OE*, *mir528*, and *SPL9 OE/mir528* lines using a western blot. Actin was probed as a loading control.

Vector Construction and Rice Transformation

The coding sequence of *SPL9* was amplified using RT–PCR and then cloned into the *pCam2300:Actin1:OCS* vector to generate the *pCam2300:Actin1:SPL9* and *pCam2300:Actin1:FLAG-SPL9* constructs. The *spl9* CRISPR/Cas9 knockout construct was constructed as previously described (Miao et al., 2013). These constructs were transformed into rice using *Agrobacterium tumefaciens*-mediated transformation (BioRun, Wuhan, China, and BIOGLE Genetech, Hangzhou, China), and were validated by sequencing in both directions. All primers used in this assay are listed in Supplemental Data 2.

Western Blotting

Equal weights of rice leaves (harvested at about 2 p.m.) were homogenized in liquid nitrogen and proteins were extracted using Laemmli 2× buffer (4% SDS, 20% glycerol, 10% 2-mercaptoethanol, 0.004% bromophenol blue, and 0.125 M Tris–HCl) (Cold Spring Harbor Protocols). The protein samples were boiled at 95°C for 10 min and separated using SDS–PAGE. The proteins were then transferred to NC membranes and hybridized with rabbit polyclonal antibodies against SPL9 (peptide EADIRELKGYHRR; the anti-

sera were affinity purified by WuXi AppTec, Shanghai, China), FLAG (Sigma-Aldrich, St. Louis, MO, USA), RSV-CP (Fu et al., 2018) (from Dr. Xueping Zhou), or actin (Kangwei Shiji, CWBIO, Beijing, China).

RNA Extraction and qPCR Analysis

Total RNA was extracted from rice plants (harvested at about 2 p.m.) using TRIzol Reagent (Thermo Fisher Scientific, Waltham, MA, USA), according to the manufacturer's instructions. The total RNA was digested with RQ1 RNase-free DNase (Promega, Madison, WI, USA) to remove any genomic DNA, after which a 2-μg aliquot of the RNA was reverse transcribed using M-MLV Reverse Transcriptase (Promega) and oligo(dT)15 primers, according to the manufacturer's instructions. The resulting cDNA was used for the qPCR reactions, which were performed using SYBR Green Real-Time PCR Master Mix (Toyobo, Osaka, Japan), following the manufacturer's instructions. *EF1a* expression was used as the internal control. For quantification of the miRNAs, a Mir-X miRNA qRT–PCR SYBR Kit (Takara Bio, Kusatsu, Japan) was used. The RNAs were polyadenylated and reverse transcribed using mRQ Enzyme Mix, after which qPCR was performed using the mRQ 3′ primer and an miRNA-specific 5′ primer.
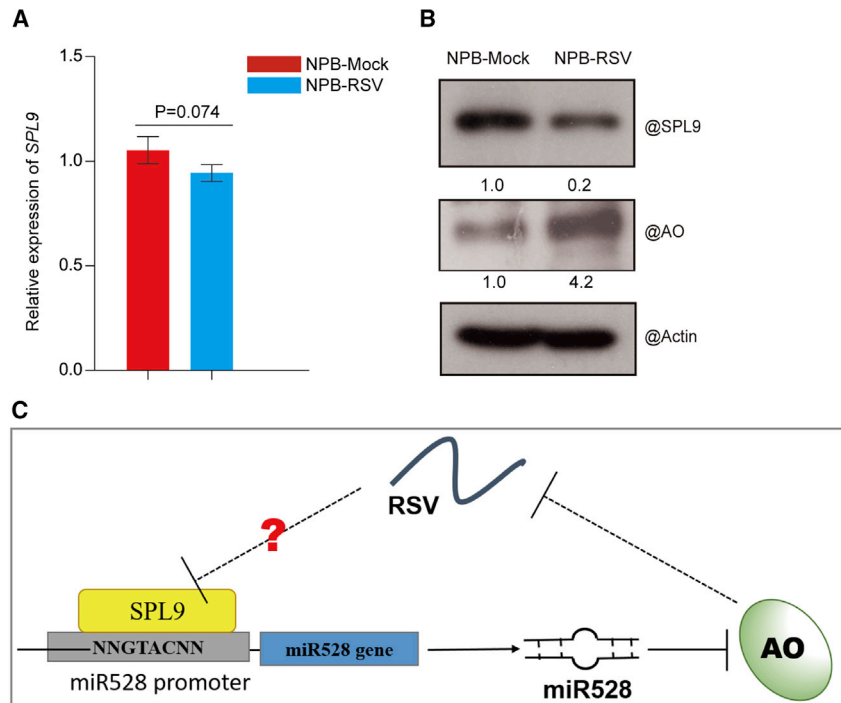
Figure 5. RSV Infection Affects the Expression of SPL9.

(A) qRT–PCR analysis of the expression level of *SPL9* in mock-inoculated or RSV-infected wild type (NPB). The average values (±SD) from three biological repeats are shown.

(B) Detection of SPL9 in mock-inoculated or RSV-infected wild type (NPB) by western blot. Actin was probed and served as a loading control.

(C) A model of the SPL9-*miR528-AO* pathway regulating plant antiviral immunity. SPL9 binds to the GTAC motif in the miR528 promoter to activate its transcription. MiR528 is loaded onto AGO1 and forms an RNA-induced silencing complex to cleave the target, *AO*, and thus regulates the rice response to RSV infection.

protein (SPL9 SBP-GST) in Transetta cells (DE3; TransGen Biotech, Beijing, China). The fusion proteins were purified using glutathione Sepharose 4B beads (GE Healthcare). The primers used for the amplification of SPL9 SBP are listed in Supplemental Data 2. Oligonucleotide probes containing GTAC motifs were synthesized and labeled with biotin (Ruibio, Beijing, China). An EMSA was performed using the Chemiluminescent EMSA Kit (Thermo Fisher Scientific). The probe sequences are shown in Supplemental Data 2.

U6 was used as the internal control. The primers used are listed in Supplemental Data 2.

Y1H Assay

The miR528 promoter region containing the GTAC motifs was cloned into the *pHis2* vector (Clontech) to generate the reporter construct miR528*pro:His*. The GTAC motifs in the miR528 promoter were also mutated into GATC to generate a mutant miR528 promoter, which was cloned into the *pHis2* vector to generate the reporter construct miR528*promut:His*. To generate the AD-SPLs, the full-length coding sequences of SPL1–19 were individually amplified using PCR and cloned into the *pGADT7Rec2* vector (Clontech), which contains Leu and Trp biosynthesis genes (Takara Bio). The individual AD-SPLs were separately co-transformed into the yeast strain Y187 alongside the reporter construct. The transformants were then grown on SD/-Trp-Leu and SD/-Trp-Leu-His dropout medium for selection or the activation test. The primers used are listed in Supplemental Data 2.

Dual-Luciferase Reporter System

One kilobase of miR528 promoter or mutant miR528 promoter, in which all GTAC motifs were mutated into GATC, was inserted into the *pGreen II 0800-LUC* vector and used as a reporter construct (Zhang et al., 2014).The coding sequence of SPL9 was inserted into *pCambia2300* and used as an effector construct. *Agrobacterium* strain GV3101 carrying the reporter plasmid (miR528pro:LUC or miR528pro mut:LUC) and a specific effector plasmid (empty vector *pCambia2300* or *pCambia2300-SPL9*) was cultured to OD_{600} = 0.5 and infiltrated into *Nicotiana benthamiana* leaves. The dual-luciferase reporter system (Promega) was used to analyze the transient expression in *N. benthamiana* leaves 2 days after infiltration. The activities of firefly and Renilla luciferases were measured on a GLO-MAX 20/20 luminometer (Promega). The ratio of firefly to Renilla was calculated to indicate the final transcriptional activity.

Protein Expression and Purification, and EMSAs

The DNA-binding domain of SPL9 (SPL9 SBP) was amplified using PCR, then inserted into the *pGEX4T1* vector (GE Healthcare, Chicago, IL, USA) and expressed as a glutathione *S*-transferase fusion

ChIP–qPCR

A 2-g sample of 2-week-old *FLAG-SPL9-OE* rice leaves was ground to powder in liquid nitrogen and crosslinked with 1% (v/v) formaldehyde for 10 min. The crosslinking reaction was stopped using 0.125 M glycine, after which the nuclei were isolated and sonicated. ANTI-FLAG Affinity Gel (Sigma-Aldrich) was used to immunoprecipitate the protein–DNA complexes, which were then recovered and dissolved in water as DNA templates. A qPCR was performed to test the enrichment of promoter regions by SPL9. Chromatin precipitated without any antibodies was used as a negative control while the chromatin isolated before precipitation was used as an input control. The primers used are listed in Supplemental Data 2.

MST Assay

The MST assay was performed according to the manufacturer's instructions as previously described to dertermine the binding constant between SPL9 and miR528 promoter. (Jerabek-Willemsen et al., 2014; Jin et al., 2016). In SPL9 SBP/miR528 promoter interaction assays, a region of the miR528 promoter containing a GTAC motif was labeled with FAM, and was held at a constant concentration while the concentrations of SPL9-SBP or GST were gradient diluted. After a short incubation in MST buffer, the samples were loaded into MST-standard glass capillaries. The measurements were performed at 25°C using 20% LED power and 20% MST power in an MST machine (NanoTemper Technologies; München, Germany). The assays were repeated three times for each affinity measurement. Data analyses were performed using the Nanotemper Analysis and OriginPro 8.0 software provided by the manufacturer.

ACCESSION NUMBERS

Information regarding the genes investigated in this study is provided in Supplemental Data 3.

SUPPLEMENTAL INFORMATION

Supplemental Information is available at *Molecular Plant Online*.

AUTHOR CONTRIBUTIONS

S.Y. and Z.Y.: Conception and design, acquisition of data, analysis and interpretation of data, drafting or revising the article; Y.H., G.G., and X.K.: Acquisition of data, analysis and interpretation of data; R.Y., Y.L., T.Z., H.W., W.W., and X.C.: Acquisition of data, contribution of unpublished essential data or reagents; Y.L. and J.W., Conception and design, analysis and interpretation of data, drafting or revising the article, contribution of unpublished essential data or reagents.

REFERENCES

Baumberger, N., Tsai, C.H., Lie, M., Havecker, E., and Baulcombe, D.C. (2007). The Polerovirus silencing suppressor P0 targets ARGONAUTE proteins for degradation. Curr. Biol. **17**:1609–1614.

Brosseau, C., and Moffett, P. (2015). Functional and genetic analysis identify a role for *Arabidopsis* ARGONAUTE5 in antiviral RNA silencing. Plant Cell **27**:1742–1754.

Carbonell, A., and Carrington, J.C. (2015). Antiviral roles of plant ARGONAUTES. Curr. Opin. Plant Biol. **27**:111–117.

Diaz-Pendon, J.A., Li, F., Li, W.X., and Ding, S.W. (2007). Suppression of antiviral silencing by cucumber mosaic virus 2b protein in *Arabidopsis* is associated with drastically reduced accumulation of three classes of viral small interfering RNAs. Plant Cell **19**:2053–2063.

Du, P., Wu, J., Zhang, J., Zhao, S., Zheng, H., Gao, G., and Li, Y. (2011). Viral infection induces expression of novel phased microRNAs from conserved cellular microRNA precursors. PLoS Pathog. **7**:e1002176.

Du, Z., Chen, A., Chen, W., Westwood, J.H., Baulcombe, D.C., and Carr, J.P. (2014). Using a viral vector to reveal the role of microRNA159 in disease symptom induction by a severe strain of Cucumber mosaic virus. Plant Physiol. **164**:1378–1388.

Fang, X., and Qi, Y. (2016). RNAi in plants: an Argonaute-centered view. Plant Cell **28**:272–285.

Fu, S., Xu, Y., Li, C., Li, Y., Wu, J., and Zhou, X. (2018). Rice stripe virus interferes with S-acylation of remorin and induces its autophagic degradation to facilitate virus infection. Mol. Plant **11**:269–287.

Guo, Z., Li, Y., and Ding, S.W. (2019). Small RNA-based antimicrobial immunity. Nat. Rev. Immunol. **19**:31–44.

Hanemian, M., Barlet, X., Sorin, C., Yadeta, K.A., Keller, H., Favery, B., Simon, R., Thomma, B.P., Hartmann, C., Crespi, M., et al. (2016). *Arabidopsis* CLAVATA 1 and CLAVATA 2 receptors contribute to *Ralstonia solanacearum* pathogenicity through a miR169-dependent pathway. New Phytol. **211**:502–515.

Huang, Y., and Li, Y. (2018). Secondary siRNAs rescue virus-infected plants. Nat. Plants **4**:136.

Jerabek-Willemsen, M., André, T., Wanner, R., Roth, H.M., Duhr, S., Baaske, P., and Breitsprecher, D. (2014). MicroScale thermophoresis: interaction analysis and beyond. J. Mol. Struct. **1077**:101–113.

Jin, L., Qin, Q., Wang, Y., Pu, Y., Liu, L., Wen, X., Ji, S., Wu, J., Wei, C., Ding, B., et al. (2016). Rice dwarf virus P2 protein hijacks auxin signaling by directly targeting the rice OsIAA10 protein, enhancing viral infection and disease development. PLoS Pathog. **12**:e1005847.

Liu, J., Cheng, X., Liu, D., Xu, W., Wise, R., and Shen, Q.H. (2014). The miR9863 family regulates distinct Mla alleles in barley to attenuate NLR receptor-triggered disease resistance and cell-death signaling. PLoS Genet. **10**:e1004755.

Ma, Z., and Zhang, X. (2018). Actions of plant Argonautes: predictable or unpredictable? Curr. Opin. Plant Biol. **45**:59–67.

Miao, J., Guo, D., Zhang, J., Huang, Q., Qin, G., Zhang, X., and Qu, L.J. (2013). Targeted mutagenesis in rice using CRISPR-Cas system. Cell Res. **23**:1233.

Navarro, L., Dunoyer, P., Jay, F., Arnold, B., Dharmasiri, N., Estelle, M., Voinnet, O., and Jones, J.D. (2006). A plant miRNA contributes to antibacterial resistance by repressing auxin signaling. Science **312**:436–439.

Ouyang, S., Park, G., Atamian, H.S., Han, C.S., Stajich, J.E., Kaloshian, I., and Borkovich, K.A. (2014). MicroRNAs suppress NB domain genes in tomato that confer resistance to *Fusarium oxysporum*. PLoS Pathog. **10**:e1004464.

Qu, F., Ye, X., and Morris, T.J. (2008). *Arabidopsis* DRB4, AGO1, AGO7, and RDR6 participate in a DCL4-initiated antiviral RNA silencing pathway negatively regulated by DCL1. Proc. Natl. Acad. Sci. U S A **105**:14732–14737.

Sanei, M., and Chen, X. (2015). Mechanisms of microRNA turnover. Curr. Opin. Plant Biol. **27**:199–206.

Tang, J., and Chu, C. (2017). MicroRNAs in crop improvement: fine-tuners for complex traits. Nat. Plants **3**:17077.

Wang, H., Jiao, X., Kong, X., Hamera, S., Wu, Y., Chen, X., Fang, R., and Yan, Y. (2016). A signaling cascade from miR444 to RDR1 in rice antiviral RNA silencing pathway. Plant Physiol. **170**:2365–2377.

Wang, Q., Liu, Y., He, J., Zheng, X., Hu, J., Liu, Y., Dai, H., Zhang, Y., Wang, B., Wu, W., et al. (2014). STV11 encodes a sulphotransferase and confers durable resistance to rice stripe virus. Nat. Commun. **5**:4768.

Wang, Q.L., Sun, A.Z., Chen, S.T., Chen, L.S., and Guo, F.Q. (2018a). SPL6 represses signalling outputs of ER stress in control of panicle cell death in rice. Nat. Plants **4**:280–288.

Wang, Z., Xia, Y., Lin, S., Wang, Y., Guo, B., Song, X., Ding, S., Zheng, L., Feng, R., Chen, S., et al. (2018b). Osa-miR164a targets OsNAC 60 and negatively regulates rice immunity against the blast fungus *Magnaporthe oryzae*. Plant J. **95**:584–597.

Wang, J., Zhou, L., Shi, H., Chern, M., Yu, H., Yi, H., He, M., Yin, J., Zhu, X., Li, Y., et al. (2018c). A single transcription factor promotes both yield and immunity in rice. Science **361**:1026–1028.

Wang, S., Li, S., Liu, Q., Wu, K., Zhang, J., Wang, S., Wang, Y., Chen, X., Zhang, Y., Gao, C., et al. (2015). The OsSPL16-GW7 regulatory module determines grain shape and simultaneously improves rice yield and grain quality. Nat. Genet. **47**:949–954.

Wu, J., Yang, R., Yang, Z., Yao, S., Zhao, S., Wang, Y., Li, P., Song, X., Jin, L., Zhou, T., et al. (2017). ROS accumulation and antiviral defence control by microRNA528 in rice. Nat. Plants **3**:16203.

Wu, J., Yang, Z., Wang, Y., Zheng, L., Ye, R., Ji, Y., Zhao, S., Ji, S., Liu, R., Xu, L., et al. (2015). Viral-inducible Argonaute18 confers

broad-spectrum virus resistance in rice by sequestering a host microRNA. Elife **4**:e05733.

Xie, K., Wu, C., and Xiong, L. (2006). Genomic organization, differential expression, and interaction of SQUAMOSA promoter-binding-like transcription factors and microRNA156 in rice. Plant Physiol. **142**:280–293.

Xu, W., Meng, Y., and Wise, R.P. (2014). Mla- and Rom1- mediated control of microRNA398 and chloroplast copper/zinc superoxide dismutase regulates cell death in response to the barley powdery mildew fungus. New Phytol. **201**:1396–1412.

Yamasaki, H., Hayashi, M., Fukazawa, M., Kobayashi, Y., and Shikanai, T. (2009). SQUAMOSA promoter binding protein-like7 is a central regulator for copper homeostasis in *Arabidopsis*. Plant Cell **21**:347–361.

Yang, Z., and Li, Y. (2018). Dissection of RNAi-based antiviral immunity in plants. Curr. Opin. Virol. **32**:88–99.

Zhang, C., Ding, Z., Wu, K., Yang, L., Li, Y., Yang, Z., Shi, S., Liu, X., Zhao, S., Yang, Z., et al. (2016). Suppression of jasmonic acid-mediated defense by viral-inducible MicroRNA319 facilitates virus infection in rice. Mol. Plant **9**:1302–1314.

Zhang, X., Zhu, Z., An, F., Hao, D., Li, P., Song, J., Yi, C., and Guo, H. (2014). Jasmonate-activated MYC2 represses ETHYLENE INSENSITIVE3 activity to antagonize ethylene-promoted apical hook formation in *Arabidopsis*. Plant Cell **26**:1105–1117.

Zhang, X., Zhao, H., Gao, S., Wang, W.C., Katiyar-Agarwal, S., Huang, H.D., Raikhel, N., and Jin, H. (2011). *Arabidopsis* Argonaute 2 regulates innate immunity via miRNA393*-mediated silencing of a Golgi-localized SNARE gene, MEMB12. Mol. Cell **42**:356–366.

Zheng, L., Zhang, C., Shi, C., Wang, Y., Zhou, T., Sun, F., Wang, H., Zhao, S., Qin, Q., Qiao, R., et al. (2017). Rice stripe virus NS3 protein regulates primary miRNA processing through association with the miRNA biogenesis factor OsDRB1 and facilitates virus infection in rice. PLoS Pathog. **13**:e1006662.